

EXCLUSIVE AND INCLUSIVE WEAK DECAYS
OF THE B -MESON^a

I.L. Grach⁽¹⁾, I.M. Narodetskii⁽¹⁾, S. Simula⁽²⁾ and K.A. Ter-Martirosyan⁽¹⁾

⁽¹⁾Institute for Theoretical and Experimental Physics, 117259 Moscow, Russia

⁽²⁾Istituto Nazionale di Fisica Nucleare, Sezione Sanità,
Viale Regina Elena 299, I-00161 Roma, Italy

Abstract

A relativistic quark model is applied to the description of semileptonic and non-leptonic charmed decays of the B -meson. The exclusive semileptonic modes $B \rightarrow D\ell\nu_\ell$ and $B \rightarrow D^*\ell\nu_\ell$ are described through the universal Isgur-Wise form factor, which is calculated in terms of a constituent quark model wave function for the B -meson. Different approximations for the latter, either based on a phenomenological ansatz or derived from analyses of the meson spectra, are adopted. In particular, two wave functions, constructed via the Hamiltonian light-front formalism using a relativized and a non-relativistic constituent quark model, are considered, obtaining a link between standard spectroscopic quark models and the B -meson decay physics. The inclusive semileptonic and non-leptonic branching ratios are calculated within a convolution approach, inspired by the partonic model and involving the same B -meson wave function used for the evaluation of the exclusive semileptonic modes. Our results for the major branching ratios are consistent with available experimental data and the sum of all the calculated branching ratios turns out to be close to unity. In particular, we found that: i) a remarkable fraction ($\sim 35\%$) of semileptonic decay modes occur in non- D , non- D^* final states; ii) non-perturbative effects enhance the inclusive $b \rightarrow c\bar{u}d$ decay channels, with a sizable contribution provided by *internal* decays into heavy mesons and baryon-antibaryon pairs; the resulting reduction of the semileptonic branching ratio brings the theoretical prediction in agreement with the experimental value without increasing at the same time the charm counting.

^aTo appear in Nuclear Physics B.

1 Introduction.

The investigation of semileptonic (SL) and non-leptonic (NL) decays of the B -meson can provide relevant information on the fundamental parameters of the Standard Model of the electroweak interaction and on the internal structure of hadrons. However, the extraction of the Cabibbo-Kobayashi-Maskawa (CKM) [1] mixing parameters from the experiments requires a precise knowledge of the transition form factors relevant in the matrix elements of the weak hadronic current. In particular, the most accurate determination of the CKM matrix element $|V_{bc}|$ is presently based on the value of the $B \rightarrow D^* \ell \nu_\ell$ transition form factors near the point of zero recoil [2, 3, 4, 5], while the evaluation of the lepton spectra and branching ratios requires the knowledge of the transition form factors in their full kinematical range.

As far as the theoretical point of view is concerned, the Heavy Quark Effective Theory ($HQET$) [6] is widely recognized as a very powerful tool for investigating the decay modes of heavy flavours and, recently [7], a model-independent framework has been developed for the treatment of inclusive decays. The latter approach relies on the formalism of $HQET$ and on the use of the operator product expansion (OPE) in the physical region of time-like momenta. Thus, the hypothesis of quark-hadron duality, in its global form for SL decays and in the local one for NL processes, has to be invoked [8]. The concept of quark-hadron duality, though it has not yet been derived from first principles, is essential in the QCD phenomenology and corresponds to the assumption that the sum over many hadronic final channels eliminates bound-state effects related to the specific structure of each individual final hadron. The validity of the global duality has been tested in inclusive hadronic τ decays [9], whereas the possibility of a failure of the local duality in inclusive NL processes has been recently raised in Ref. [10]. It should be reminded that the model-independent approach of Ref. [7] has other limitations, like, e.g., the need of a (at least partial) OPE resummation in the end-point region of the predicted lepton spectrum. Moreover, though the $HQET$ provides a systematic expansion for organizing power corrections, it does not help in calculating the relevant (non-perturbative) hadronic matrix elements. Therefore, the use of the phenomenological constituent quark (CQ) model (see, e.g., [11, 12, 13]) for the description of the non-perturbative aspects of the hadron structure could be still of interest. In this respect, it is well known that the CQ model is remarkably successful in describing the non-perturbative physics of hadron mass spectra; however, a successful model of hadrons must go beyond the spectroscopy and should describe the internal structure of hadrons in order to predict, e.g., transition form factors and decay rates.

In this paper non-perturbative QCD effects are mocked up by a CQ model wave function for the B -meson. The internal motion of the b -quark inside the B -meson^b is described by a distribution function $|\chi(x, p_\perp)|^2$, which represents the probability to find the b -quark carrying a light-front (LF) fraction x of the B -meson momentum and a transverse relative momentum squared $p_\perp^2 \equiv |\vec{p}_\perp|^2$. The branching ratios of all the major decay modes of the B -meson are calculated in terms of the distribution $|\chi(x, p_\perp^2)|^2$. Thus, a relevant feature of our approach is that both exclusive and inclusive SL as well as NL decays modes are coherently treated in terms of the same b -quark distribution in the B -meson. The sensitivity of our predictions to various choices of $\chi(x, p_\perp^2)$, based on the phenomenological ansatz of Ref. [14] or derived from analyses of the meson spectra, is investigated. As to the latter case, two wave functions, constructed via the Hamiltonian LF formalism using a relativized

^bThe effects due to the bound-state structure have been firstly treated in Ref. [15] by attributing a Fermi motion to the b -quark in the B -meson.

[16] and a non-relativistic [17] CQ model, have been considered, obtaining a link between standard spectroscopic quark models and the B -meson decay physics.

As it is well known, B -meson decays occur mainly through the CKM favored $b \rightarrow c$ transition. The dominant diagrams are the so-called spectator diagrams depicted in Figs. 1 and 2. In SL decays (Fig. 1) the virtual W^- boson materializes into a lepton pair, and the c -quark and the spectator light antiquark hadronize independently of the leptonic current. In case of the exclusive SL transitions $B \rightarrow D\ell\nu_\ell$ and $B \rightarrow D^*\ell\nu_\ell$ the limit of infinite heavy-quark masses is considered, so that all the relevant matrix elements can be expressed in terms of a single universal function, the Isgur-Wise (IW) form factor [18, 19, 20]. The IW function is explicitly calculated using our CQ model wave functions of the B -meson. As for the inclusive SL decays, our approach is similar to the deep inelastic scattering (DIS) approach by Bjorken (see Refs. [21], [22] and [23]), which pictures the heavy-meson decay as the decay of its partons. A relevant feature of our approach is that the SL width is not represented as an expansion over the *small* parameter $1/m_b$, but it is related to a convolution of the free-quark decay tensor over the b -quark distribution $|\chi(x, p_\perp^2)|^2$. Though this paper deals with calculations of branching ratios, we want to point out that within our model-dependent approach both the lepton and final hadron spectra can be predicted in their whole kinematical accessible range. In this way our technique can be considered complementary to model-independent heavy-flavour methods.

The LF partonic approach can be easily extended to the description of NL decays, in which the virtual W^- boson materializes into a $\bar{u}d$ (Fig. 2a) or $\bar{c}s$ (Fig. 2b) pairs; the produced quark pair becomes one of the final hadrons, while the c -quark couples with the spectator light antiquark to form other hadrons. However, the spectator diagram is modified by the exchange of hard gluons between initial and final quark lines. Indeed, NL heavy-flavour decays are described by the effective Lagrangian of Ref. [24], which contains both colour-singlet and colour-octet four-fermion operators mixing under QCD renormalization group equations. We will refer to the contributions of these two kind of operators as the *external* and *internal* NL transitions, respectively, the latter being characterized by a different set of quark pairing in the final hadrons, as it is depicted in Fig. 3. The NL branching ratios are estimated both adopting the so-called factorization approximation for the matrix elements of the weak effective Lagrangian and neglecting the perturbative QCD corrections specific for each given channel. Only the corrections due to hard-gluon exchange, yielding the effective Lagrangian of Ref. [24], are taken into account (see also [15, 25, 26]). We stress again that in our approach both SL and NL B -meson decays are described in terms of the same (model-dependent) bound-state wave function of the B -meson, $\chi(x, p_\perp^2)$.

The plan of the paper is as follows. In Section 2 the CQ models adopted for the description of the B -meson wave function are briefly presented and the IW form factor is calculated. Section 3 contains the application of our approach to the evaluation of both exclusive and inclusive SL B -meson decays. In Section 4 our treatment of *external* and *internal* NL decays is presented. All the results for the branching ratios, calculated using our CQ models of the B -meson wave function, are reported in Section 5. It is shown that an overall reproduction of the available data can be achieved and the sum of all the calculated branching ratios turns out to be very close to unity. Moreover, we found that: i) a remarkable fraction ($\sim 35\%$) of SL decay modes occur in non- D , non- D^* final states; ii) non-perturbative effects enhance the inclusive $b \rightarrow \bar{c}ud$ decay channels, with a sizable contribution provided by decays into heavy mesons and baryon-antibaryon pairs; the resulting reduction of the SL branching ratio brings the theoretical prediction in agreement with the experimental value without increasing at the same time the charm counting (i.e., the number of charm

quarks produced per b -quark decay). Finally, Section 6 contains our conclusions.

2 The Isgur-Wise function.

In the limit of infinite heavy-quark masses all the relevant matrix elements of the flavour-changing vector and axial-vector currents, $V_\mu = (\bar{c}\gamma_\mu b)$ and $A_\mu = (\bar{c}\gamma_\mu\gamma_5 b)$, are related to a single form factor, the IW function $\xi(\eta)$, which depends only on the product η of the four-velocities of the initial and final hadrons. The $HQET$ allows to write the matrix elements for pseudoscalar (PS) to PS and PS to vector (V) meson transitions as follows (cf. [6])

$$\langle D|V_\mu|B \rangle = \sqrt{M_B M_D} \xi(\eta) (v + v_D)_\mu \quad (1)$$

$$\langle D^*, \lambda|V_\mu|B \rangle = \sqrt{M_B M_{D^*}} \xi(\eta) \varepsilon_{\mu\nu\rho\sigma} v^\nu v_{D^*}^\sigma e^{\nu*}(\lambda) \quad (2)$$

$$\langle D^*, \lambda|A_\mu|B \rangle = \sqrt{M_B M_{D^*}} \xi(\eta) [e_\mu(\lambda)(1 + \eta) - v_{D^*\mu}(v \cdot e(\lambda))] \quad (3)$$

where M_B (M_j) and v (v_j) are the mass and four-velocity of the initial (final) heavy meson ($j = D, D^*$) and $e(\lambda)$ is the polarization four-vector of the final vector meson with helicity λ . As is known, the dimensionless variable $\eta \equiv v \cdot v_j$ is related to the four-momentum transfer $q = P_B - P_j = M_B v - M_j v_j$ by $\eta = (M_B^2 + M_j^2 - q^2)/2M_B M_j = (1 + \zeta_j^2 - q^2/M_B^2)/2\zeta_j$, where $\zeta_j \equiv M_j/M_B$. In the limit $m_{b,c} \rightarrow \infty$ the normalization of $\xi(\eta)$ is $\xi(1) = 1$ and the leading non-perturbative corrections are quadratic in $1/m_{b,c}$ thanks to the Luke's theorem [27], which is the analog of the Ademollo-Gatto theorem [28] in case of the heavy-quark symmetry.

In Ref. [29] the IW function has been calculated in the infinite momentum frame (IMF). Choosing the z axis along the direction of the Lorentz boost, one defines the invariant $1 - \gamma \equiv q^+/P_B^+ = (q_0 + q_z)/(P_{B0} + P_{Bz})$; it can be easily verified that $q^2 = (1 - \gamma)(M_B^2 - M_j^2/\gamma)$ and $\eta = \frac{1}{2}(\frac{\gamma}{\zeta_j} + \frac{\zeta_j}{\gamma})$. Then, in terms of the IMF variables x and p_\perp^2 (where x is the fraction of the longitudinal B -meson momentum carried by the b -quark and p_\perp^2 its transverse momentum squared) the explicit expression for $\xi(\eta)$ is [29]

$$\xi(\eta) = \int d\vec{p}_\perp \int_0^\gamma dx_{sp} \chi(1 - x_{sp}, p_\perp^2) \chi(1 - \frac{x_{sp}}{\gamma}, p_\perp^2) \left[1 + \frac{(v + v_j) \cdot v_{sp}}{1 + \eta} \right] \quad (4)$$

where $x_{sp} \equiv 1 - x$, v_{sp} is the four-velocity of the spectator quark and $\chi(x, p_\perp^2)$ is the heavy-meson wave function. In refs. [29, 14] a simple exponential ansatz has been considered, which in terms of the IMF variables x and p_\perp^2 reads as

$$\chi_{ph}(x, p_\perp^2) = \frac{\mathcal{N}}{\sqrt{1-x}} \exp \left[-\frac{\lambda_0}{2} \left(\frac{1-x}{\xi_0} + \frac{\xi_0}{1-x} + \frac{\xi_0 p_\perp^2}{(1-x)m_{sp}^2} \right) \right] \quad (5)$$

where $\xi_0 \equiv m_{sp}/M_B$, m_{sp} is the mass of the light spectator-quark, λ_0 is an adjustable parameter and \mathcal{N} is a normalization constant fixed by the condition $\int d\vec{p}_\perp dx |\chi(x, p_\perp^2)|^2 = 1$. Using Eq. (5) in Eq. (4), the IW form factor is explicitly given by (cf. [29])

$$\xi_{ph}(\eta) = \frac{2 K_1(\lambda_0 r) + \frac{2}{r} K_2(\lambda_0 r)}{r K_1(2\lambda_0) + K_2(2\lambda_0)} \quad (6)$$

where $r = \sqrt{2(1+\eta)}$ and $K_{1,2}$ are modified Bessel functions.

A relativistic approach to the construction of CQ model wave functions of mesons is provided by the Hamiltonian LF formalism [30], where the intrinsic wave function, satisfying the correct transformation properties under LF boosts, has the following structure (see, e.g., Refs. [31, 32, 33])

$$\Psi_{LF}(\vec{p}_\perp, x; \nu\bar{\nu}) = \sqrt{\frac{M_0}{4x(1-x)}} \left[1 - \left(\frac{m_b^2 - m_{sp}^2}{M_0^2} \right)^2 \right] \frac{w(p^2)}{\sqrt{4\pi}} \mathcal{R}(\vec{p}_\perp, x; \nu, \bar{\nu}) \quad (7)$$

where m_b is the mass of the b -quark, M_0 is the free mass operator $M_0^2 = (p_\perp^2 + m_b^2)/x + (p_\perp^2 + m_{sp}^2)/(1-x)$ and the momentum dependent quantity $\mathcal{R}(\vec{p}_\perp, x; \nu\bar{\nu})$ arises from the relativistic composition of the quark-spin wave functions, with $\nu, \bar{\nu} = \pm 1/2$ being the spin projection variables of the quarks. In Eq. (7) $p^2 \equiv p_\perp^2 + p_n^2$, where p_n is the longitudinal momentum defined as $p_n = (x - \frac{1}{2})M_0 + (m_{sp}^2 - m_b^2)/2M_0$ and the free-mass M_0 acquires the familiar form $M_0 = \sqrt{m_b^2 + p^2} + \sqrt{m_{sp}^2 + p^2}$.

The LF wave function (7) is eigenfunction of the mass operator $\mathcal{M} = M_0 + \mathcal{V}$, where \mathcal{V} is a Poincaré-invariant interaction term. As explained in Refs. [31, 32, 33], the transformed mass operator $\mathcal{R}\mathcal{M}\mathcal{R}^\dagger$ can be identified with any semi-relativistic effective $q\bar{q}$ Hamiltonian able to reproduce meson mass spectra. In this paper, for the latter we will consider two choices. In the first one, the radial wave function $w(p^2)$, appearing in Eq. (7), is the solution of the following wave equation

$$\left[\sqrt{m_b^2 + p^2} + \sqrt{m_{sp}^2 + p^2} + V_{GI} \right] w(p^2)|00\rangle = M_{PS} w(p^2)|00\rangle \quad (8)$$

where M_{PS} is the mass of the PS meson, $|00\rangle = \sum_{\nu\bar{\nu}} \langle \frac{1}{2}\nu \frac{1}{2}\bar{\nu} | 00 \rangle | \frac{1}{2}\nu \rangle | \frac{1}{2}\bar{\nu} \rangle$ is the canonical quark-spin wave function, and V_{GI} is the effective potential elaborated by Godfrey and Isgur (GI) in Ref. [16]. The second choice is represented by the non-relativistic (NR) Hamiltonian of Ref. [17], viz.

$$\left[m_b + m_{sp} + \frac{p^2}{2\mu} + V_{NR} \right] w(p^2)|00\rangle = M_{PS} w(p^2)|00\rangle \quad (9)$$

where $\mu \equiv m_{sp}m_b/(m_{sp}+m_b)$. Note that both the relativized V_{GI} and the non-relativistic V_{NR} effective interactions are composed by a linear-confining part (dominant at large separations) and an effective one-gluon-exchange (OGE) term (dominant at short separations), which is responsible for the hyperfine splitting of meson mass spectra.

Within the LF formalism the function $\chi(x, p_\perp^2)$ entering Eq. (4) can be written in terms of the radial wave function $w(p^2)$ as (cf. also Ref. [33])

$$\chi^{LF}(x, p_\perp^2) = \sqrt{\frac{M_0}{4x(1-x)}} \left[1 - \left(\frac{m_b^2 - m_{sp}^2}{M_0^2} \right)^2 \right] \frac{w(p^2)}{\sqrt{4\pi}} \quad (10)$$

We also define the distribution function $F(x)$ as the probability of finding the b -quark carrying a fraction x of the B -meson momentum, viz.

$$F(x) = \int d\vec{p}_\perp \sum_{\nu\bar{\nu}} \Psi_{LF}^\dagger(\vec{p}_\perp, x; \nu\bar{\nu}) \Psi_{LF}(\vec{p}_\perp, x; \nu\bar{\nu}) = \int d\vec{p}_\perp |\chi^{LF}(x, p_\perp^2)|^2 \quad (11)$$

with $\int_0^1 dx F(x) = 1$. In what follows, we will refer to the phenomenological ansatz χ_{ph} (Eq. (5)) as case *A* and to the *LF* wave functions χ_{GI}^{LF} and χ_{NR}^{LF} , obtained from Eq. (10) using the solutions of Eqs. (8) and (9), as cases *B* and *C*, respectively. The values adopted for the constituent quark masses are collected in Table 1.

In Fig. 4 the *b*-quark distribution function $F(x)$, calculated for the three cases *A*, *B* and *C*, is shown. It can be seen that quite similar results are obtained using χ_{ph} and χ_{NR}^{LF} , whereas the wave function χ_{GI}^{LF} , obtained from the relativized *GI* interaction, yields a broader *x*-distribution with the location of the peak shifted to little bit higher values of *x*. Such differences are due to the larger content of high-momentum components, generated by the *OGE* term of the *GI* interaction (see Refs. [31, 32]), and to the lower value of the *u* (*d*) constituent quark mass (see Table 1). The results obtained for the *IW* form factor (Eq. (6) in case *A* and Eq. (4) for cases *B* and *C*), multiplied by $|V_{bc}| = 0.0390$ [5], are plotted in Fig. 5 and compared with the experimental data of Refs. [34, 35, 36]. All the three model wave functions yield a *IW* form factor which is consistent with measurements; however, present experimental uncertainties are too large to allow a stringent test on the model wave function. The calculated slope of the *IW* function, $\rho^2 \equiv -d\xi(\eta)/d\eta|_{\eta=1}$, is: 1.13 (case *A*), 1.03 (case *B*) and 1.22 (case *C*).

3 Semileptonic decays.

In this section the formulae used for the calculation of both exclusive and inclusive *SL* widths are reported. The main approximations involved are the use of the Heavy Quark Symmetry (*HQS*) for the exclusive modes (see Eqs. (1-3)) and the partonic approximation for the inclusive modes (see Refs. [14, 21, 22, 23]). Within our approach the *SL* width is not represented as an expansion over the *small* parameter $1/m_b$, but it related to a convolution of the free-quark decay tensor over our model-dependent *b*-quark distribution $|\chi(x, \vec{p}_\perp^2)|^2$. The same bound-state wave function is used for both the exclusive and the inclusive channels. Moreover, as it will be shown in the Section 4, our formulae for the *SL* decays can be easily adapted to the calculation of *NL* modes, where non-perturbative bound-state effects might play a different role.

3.1 Semileptonic decays $B \rightarrow D\ell\nu_\ell$ and $B \rightarrow D^*\ell\nu_\ell$.

The double-differential decay width for the exclusive semileptonic process $B \rightarrow j\ell\nu_\ell$, where $j = D$ or $j = D^*$, can be cast into the following form (cf. [7, 14])

$$\frac{d\Gamma_{j\ell\nu_\ell}}{dq^2 dE_\ell} = \frac{G_F^2 |V_{bc}|^2}{64\pi^3} L_{\alpha\beta} \bar{W}_{\alpha\beta}^j \quad (12)$$

where q^2 is the four-momentum squared of the dilepton system and $E_\ell \equiv p_\ell \cdot v$ is the charged lepton energy in the *B*-meson rest frame. In Eq. (12) $L_{\alpha\beta}$ is the leptonic tensor, given explicitly by

$$\begin{aligned} L_{\alpha\beta} &= \frac{1}{4} \sum_{spins} (\bar{\ell} \gamma_\alpha (1 - \gamma_5) \nu_\ell) (\bar{\nu}_\ell \gamma_\beta (1 - \gamma_5) \ell) \\ &= 2 \left[p_{\ell\alpha} p_{\nu_\ell\beta} + p_{\nu_\ell\alpha} p_{\ell\beta} - g_{\alpha\beta} (p_\ell \cdot p_{\nu_\ell}) - i\varepsilon_{\alpha\beta\gamma\delta} p_\ell^\gamma p_{\nu_\ell}^\delta \right] \end{aligned} \quad (13)$$

and $\bar{W}_{\alpha\beta}^j$ is the (reduced) hadronic tensor, which involves five structure functions, \bar{W}_1^j to \bar{W}_5^j , viz.

$$\begin{aligned}\bar{W}_{\alpha\beta}^j &= \frac{1}{M_B^2} \sum_{\lambda} (j, \lambda | J_{\alpha}^{(h)} | B) (j, \lambda | J_{\beta}^{(h)} | B)^* \\ &= -g_{\alpha\beta} \bar{W}_1^j + v_{\alpha} v_{\beta} \bar{W}_2^j - i\varepsilon_{\alpha\beta\gamma\delta} v^{\gamma} u^{\delta} \bar{W}_3^j + \\ &\quad (v_{\alpha} u_{\beta} + u_{\alpha} v_{\beta}) \bar{W}_4^j + u_{\alpha} u_{\beta} \bar{W}_5^j\end{aligned}\quad (14)$$

where $u_{\alpha} \equiv q_{\alpha}/M_B$ and $J_{\alpha}^{(h)}$ is the charged weak hadronic current. Adopting the *HQS* limit for the hadronic matrix elements $(j, \lambda | J_{\alpha}^{(h)} | B)$ (see Eqs. (1-3)), one gets

$$\begin{aligned}\bar{W}_1^D &= 0, & \bar{W}_1^{D*} &= 2\zeta_{D^*}\eta (1 + \eta) \xi^2(\eta) \\ \bar{W}_2^D &= \frac{(1 + \zeta_D)^2}{\zeta_D} \xi^2(\eta), & \bar{W}_2^{D*} &= \frac{4\zeta_{D^*}\eta - (1 - \zeta_{D^*})^2}{\zeta_{D^*}} \xi^2(\eta) \\ \bar{W}_3^D &= 0, & \bar{W}_3^{D*} &= 2(1 + \eta) \xi^2(\eta) \\ \bar{W}_4^D &= -\frac{(1 + \zeta_D)}{\zeta_D} \xi^2(\eta), & \bar{W}_4^{D*} &= \frac{(1 - \zeta_{D^*} - 2\zeta_{D^*}\eta)}{\zeta_{D^*}} \xi^2(\eta) \\ \bar{W}_5^D &= \frac{1}{\zeta_D} \xi^2(\eta), & \bar{W}_5^{D*} &= -\frac{1}{\zeta_{D^*}} \xi^2(\eta)\end{aligned}\quad (15)$$

The integration over the lepton energy E_{ℓ} as well as the remaining trace of the leptonic (13) and hadronic (14) tensors can be easily performed in the general case of non-vanishing lepton masses; the final result for the exclusive *SL* decay rate, $B \rightarrow j\ell\nu_{\ell}$, is

$$\frac{d\Gamma_{j\ell\nu_{\ell}}}{d\eta} = \frac{4}{3} \Gamma_0 \Phi_{\ell} \zeta_j^3 (1 + \eta) (\eta^2 - 1)^{1/2} F^{(j)}(\eta) \xi^2(\eta) \quad (16)$$

where $\Phi_{\ell} = \sqrt{1 - 2\lambda_+ + \lambda_-^2}$, $\lambda_{\pm} = (m_{\ell}^2 \pm m_{\nu_{\ell}}^2)/q^2$, with m_{ℓ} and $m_{\nu_{\ell}}$ being the lepton masses, and

$$\begin{aligned}F^{(D)}(\eta) &= (1 + \zeta_D)^2 (\eta - 1) (1 + \lambda_1) + 3\lambda_2 (1 + \zeta_D^2 - 2\zeta_D \eta) \\ F^{(D^*)}(\eta) &= \left[(1 - \zeta_{D^*})^2 (1 + 5\eta) - 8\zeta_{D^*} \eta (\eta - 1) \right] (1 + \lambda_1) - \\ &\quad 3\lambda_2 (1 + 2\eta) (1 + \zeta_{D^*}^2 - 2\zeta_{D^*} \eta)\end{aligned}\quad (17)$$

where $\Gamma_0 \equiv G_F^2 |V_{bc}|^2 M_B^5/64\pi^3$, $\lambda_1 = \lambda_+ - 2\lambda_-^2$ and $\lambda_2 = \lambda_+ - \lambda_-^2$. In case of vanishing lepton masses ($m_{\ell} = m_{\nu_{\ell}} = 0$) Eqs. (16-17) simplify to the well known result [11]

$$\begin{aligned}\frac{d\Gamma_{D\ell\nu_{\ell}}}{d\eta} &= \frac{4}{3} \Gamma_0 \zeta_D^3 (1 + \zeta_D)^2 (\eta^2 - 1)^{3/2} \xi^2(\eta) \\ \frac{d\Gamma_{D^*\ell\nu_{\ell}}}{d\eta} &= \frac{4}{3} \Gamma_0 \zeta_{D^*}^3 (\eta^2 - 1)^{1/2} (1 + \eta) \cdot \\ &\quad \left[(1 - \zeta_{D^*})^2 (1 + 5\eta) - 8\zeta_{D^*} \eta (\eta - 1) \right] \xi^2(\eta)\end{aligned}\quad (18)$$

showing that the decay rate for the $B \rightarrow D\ell\nu_{\ell}$ transition is suppressed by an additional kinematical factor $\eta - 1$ with respect to the decay into the D^* meson.

3.2 Inclusive semileptonic decays.

In this subsection our technique adopted for the calculation of inclusive SL decay processes is presented. Its main feature is the description of the decay rate in terms of the same b -quark distribution function $\chi(x, p_\perp^2)$, introduced in the previous section, without any explicit reference to a $1/m_b$ expansion. Our approach to inclusive SL transitions can be considered quite analogous to the Bjorken DIS approach (see Refs. [21, 22, 23]). As is well known (cf. [7]), the triple-differential decay width for the inclusive $B \rightarrow X_c \ell \nu_\ell$ process is given by

$$\frac{d\Gamma_{X_c \ell \nu_\ell}}{dq^2 dM_X^2 dE_\ell} = \frac{G_F^2 |V_{bc}|^2}{16\pi^3} \frac{L^{\alpha\beta} W_{\alpha\beta}}{2M_B} \quad (19)$$

where M_X is the invariant mass of the hadrons produced in the lower block of the diagram of Fig. 1 and $W_{\alpha\beta}$ is the inclusive hadronic tensor

$$W_{\alpha\beta} = \frac{(2\pi)^3}{2M_B} \sum_{spins} \sum_n \int d\tau_n (n|J_\alpha^{(h)}|B) (n|J_\beta^{(h)}|B) \quad (20)$$

with $d\tau_n$ being the n -hadron phase space. The tensor $W_{\alpha\beta}$ has a covariant decomposition analogous to the one of Eq. (14), viz.

$$W_{\alpha\beta} = -g_{\alpha\beta} W_1(t, s) + v_\alpha v_\beta W_2(t, s) - i\varepsilon_{\alpha\beta\gamma\delta} v^\gamma u^\delta W_3(t, s) + (v_\alpha u_\beta + u_\alpha v_\beta) W_4(t, s) + u_\alpha u_\beta W_5(t, s) \quad (21)$$

where the invariant (dimensionless) variables $t \equiv q^2/M_B^2$ and $s \equiv M_X^2/M_B^2$ have been introduced. After integration over the lepton energy E_ℓ and considering non-vanishing lepton masses, the differential decay rate (19) becomes

$$\frac{d\Gamma_{X_c \ell \nu_\ell}}{dt ds} = \Gamma_0 M_B \Phi_\ell(t) a(t, s) \left\{ (1 + \lambda_1) [2t W_1(t, s) + \frac{1}{6} a^2(t, s) W_2(t, s)] + t\lambda_2 [-4W_1(t, s) + W_2(t, s) + (1 + t - s) W_4(t, s) + t W_5(t, s)] \right\} \quad (22)$$

where $a(t, s) \equiv 2|\vec{q}|/M_B = \sqrt{(1 + t - s)^2 - 4t}$.

To proceed further, we consider that the B -meson is a bound state of the decaying b -quark and a light (anti)quark-spectator \bar{q}_{sp} (\bar{u} or \bar{d}). In the spirit of the partonic approach the hadronic tensor $W_{\alpha\beta}$ can be written as [14]

$$W_{\alpha\beta} = \int dx d\vec{p}_\perp |\chi(x, p_\perp^2)|^2 \frac{1}{x} L_{\alpha\beta}^{(bc)}(p_c, p_b) \delta[(p_b - q)^2 - m_c^2] \Theta(E_c) \quad (23)$$

where the tensor $L_{\alpha\beta}^{(bc)}$, describing the $b \rightarrow c$ W^- transition, is defined analogously to the lepton tensor $L_{\alpha\beta}$ of Eq. (13). In Eq. (23) the δ -function corresponds to the decay of a b -quark with longitudinal momentum xP_B and transverse momentum \vec{p}_\perp to a c -quark, and yields two roots in x , viz.

$$\delta[(p_b - q)^2 - m_c^2] = \frac{1}{M_B^2 (x_+ - x_-)} [\delta(x - x_+) + \delta(x - x_-)] \quad (24)$$

with

$$x_\pm = \frac{1}{2} \left(1 + t - s \pm \sqrt{a^2(t, s) + 4 \frac{m_c^2 + p_\perp^2}{M_B^2}} \right) \quad (25)$$

Moreover, in Eq. (23) the function $\Theta(E_c)$ has been inserted for consistency with the use of a CQ model wave function $\chi(x, p_\perp^2)$ for the b -quark distribution in the B -meson. As a matter of fact (cf. Ref. [23]), the root x_- is related to the contribution of the so-called Z -graph, arising from the negative energy components of the c -quark propagator. The integration over x leads to

$$\begin{aligned}
W_1 &= \frac{1}{M_B} \int d\vec{p}_\perp |\chi(x_+, p_\perp^2)|^2 \\
W_2 &= \frac{4}{M_B} \int d\vec{p}_\perp |\chi(x_+, p_\perp^2)|^2 \frac{x_+}{x_+ - x_-} \\
W_3 &= W_4 = -\frac{2}{M_B} \int d\vec{p}_\perp |\chi(x_+, p_\perp^2)|^2 \frac{1}{x_+ - x_-} \\
W_5 &= 0
\end{aligned} \tag{26}$$

where we have neglected the effects of the transverse momentum in the quark tensor $L_{\alpha\beta}^{(bc)}$. After substituting $W_i(t, s)$ from Eq. (26) into Eq. (22), the inclusive SL decay rate is

$$\begin{aligned}
\Gamma_{X_c \ell \nu_\ell} &= \frac{2}{3} \Gamma_0 \int_{t_{min}}^{t_{max}} dt \Phi_\ell(t) \int_{s_{min}}^{s_{max}} ds a(t, s) \int d\vec{p}_\perp |\chi(x_+, p_\perp^2)|^2 \cdot \\
&\quad [(1 + \lambda_1) \frac{x_+ a^2(t, s)}{x_+ - x_-} + 3t (1 - \lambda_-^2)]
\end{aligned} \tag{27}$$

The integration limits in (27) are related to the lepton mass m_ℓ and to the threshold value M_{th} at which the hadron continuum starts in the lower block of the diagram of Fig. 1, viz.

$$\begin{aligned}
t_{min} &= \frac{m_\ell^2}{M_B^2} \quad , \quad t_{max} = (1 - M_{th}/M_B)^2 \\
s_{min} &= \frac{M_{th}^2}{M_B^2} \quad , \quad s_{max} = (1 - \sqrt{t})^2
\end{aligned} \tag{28}$$

The values of M_{th} used in our calculations will be specified in Section 5.

4 Non-leptonic decay modes.

In contrast to SL transitions, NL processes are complicated by the quark rearrangement mechanism due to the exchange of both soft and hard gluons. The basic assumption in our calculation of the NL amplitudes is that it is possible to separate the main contribution of the soft gluons by incorporating all the long-distance QCD effects in the non-perturbative CQ bound-state wave functions. It is well known [24, 15, 25, 26] that hard-gluon exchange modifies the weak forces driving NL heavy-flavour decays; at the mass scale $\mu = M_W$ the weak Lagrangian is

$$L_W(\mu = M_W) = -\frac{4G_F}{\sqrt{2}} [V_{cb} (\bar{c}_L \gamma_\mu b_L) + V_{ub} (\bar{u}_L \gamma_\mu b_L)] \cdot [V_{ud}^* (\bar{d}_L \gamma_\mu u_L) + V_{cs}^* (\bar{s}_L \gamma_\mu c_L)] \tag{29}$$

where we have ignored the $b \rightarrow t$ coupling term. Radiative QCD corrections lead to an effective Lagrangian at the mass scale $\mu = m_b$ [24]

$$\begin{aligned}
L_W^{eff}(\mu = m_b) &= -\frac{4G_F}{\sqrt{2}} V_{cb} V_{ud}^* \left\{ C_1 (\bar{c}_L \gamma_\mu b_L) (\bar{d}_L \gamma_\mu u_L) + C_2 (\bar{d}_L \gamma_\mu b_L) (\bar{c}_L \gamma_\mu u_L) + \right. \\
&\quad \left. (\bar{d}, u) \leftrightarrow (\bar{s}, c) \right\}
\end{aligned} \tag{30}$$

which contains both a colour-singlet, $O_1 \equiv (\bar{c}_L \gamma_\mu b_L)(\bar{d}_L \gamma_\mu u_L)$, and a colour-octet, $O_2 \equiv (\bar{d}_L \gamma_\mu b_L)(\bar{c}_L \gamma_\mu u_L)$, four-fermion transition operators. The factors $C_1 \pm C_2 = C_\pm$ are the Wilson coefficients determined by renormalization group equations, which allows to move from the mass scale $\mu = M_W$ to the lower scale $\mu = m_b$. In the leading-log approximation one has $C_\pm = L^{\gamma_\pm}$, where $L = \ln(M_W/\Lambda_{QCD})/\ln(m_b/\Lambda_{QCD})$, with Λ_{QCD} being the QCD scale, and $\gamma_+ = 6/(33 - 2N_f) = -\frac{\gamma_-}{2}$. Including next-to-leading logarithmic corrections one obtains $C_1 = 1.13$ and $C_2 = -0.29$ [24, 26], showing explicitly that the Wilson coefficient C_2 is colour-suppressed (i.e., $C_2 \sim 1/N_c$, where N_c is the number of colours). In Eq. (30) the contributions of the so-called W -exchange and weak annihilation diagrams have been neglected because they are not relevant for the transitions considered (cf. [37]).

In the next two subsections we will discuss separately the *external* NL decays, proceeding via the colour-singlet operator O_1 (Fig. 2), and the *internal* NL decays related to the colour-suppressed transition operator O_2 (Fig. 3). The operators O_1 and O_2 mix each other under QCD renormalization group equations and therefore the separation among the *external* and *internal* diagrams is scale dependent. We point out that internal decays of the \bar{B}^0 -meson lead to final hadron states different from those corresponding to external decays, namely, the external decays of the \bar{B}^0 meson due to $W^- \rightarrow \bar{c}s$ transitions lead to $(\bar{c}s) + (\bar{d}c)$ final states (like, e.g., $D_s^{*-} D^{*+}$), while in case of internal decays $(\bar{d}s) + (\bar{c}c)$ states (like, e.g., $K^{*0} + J/\psi$) are produced. The same is valid for $W^- \rightarrow \bar{u}d$ transitions, where the internal decays lead to $(\bar{d}d) + (\bar{u}c)$ hadron states (like, e.g., $\rho^0 + D^{*0}$), whereas the external ones lead to $(\bar{u}d) + (\bar{d}c)$ states (like, e.g., $\rho^- + D^{*+}$)^c.

4.1 External non-leptonic decays.

First, we discuss the amplitudes of the transitions to the continuum states $X_{\bar{u}d}$ and $X_{\bar{c}s}$ in the upper blocks of Fig. 2. The corresponding decay amplitudes are obtained from the first term in L_W^{eff} (Eq. (30)) in a way quite similar to the SL case. We use the zero-order approximation in the $1/N_c$ expansion and neglect the radiative QCD corrections different from those already included in the Wilson coefficients $C_{1,2}$. In this approximation all the amplitudes for the decays $\bar{B}^0 \rightarrow X_{\bar{u}d} D^+(D^{*+})$, $\bar{B}^0 \rightarrow X_{\bar{c}s} D^+(D^{*+})$, $\bar{B}^0 \rightarrow X_{\bar{u}d} X_{\bar{d}c}$ and $\bar{B}^0 \rightarrow X_{\bar{c}s} X_{\bar{d}c}$ are proportional to the NL enhancement factor C_1 . We disregard the contribution of the second term in Eq. (30), because it is proportional to the colour-suppressed coefficient C_2 . With these simplifications the matrix elements of interest are of the same type as the ones found in the analysis of SL decays in Sec. 3. The final result reduces to replace in Eqs. (16) and (27) the factor Γ_0 with $N_c C_1^2 \Gamma_0$ and also to consider in Eq. (13) the CQ masses instead of the lepton masses.

In case of the production of a single meson (e.g. D_s, D_s^*, \dots) in the upper block of Fig. 2 the corresponding amplitudes can be obtained from Eq. (12) by substituting the leptonic current $J_\alpha^{\ell\nu\ell} = \bar{\ell}\gamma_\alpha(1 - \gamma_5)\nu_\ell$ with $J_\alpha^{PS} = f_{PS} q_\alpha$ and $J_\alpha^V = f_V M_V e_\alpha$, where f_{PS} and f_V are the coupling constants of PS and V mesons to the W -boson, respectively, and q_α is the W -boson four-momentum. Then, instead of the leptonic tensor $L_{\alpha\beta}$ of Eq. (13) one has

$$\frac{1}{4} \sum_{spins} j_\alpha^i j_\beta^i = \begin{cases} \frac{1}{4} M_{PS}^2 f_P^2 u_\alpha u_\beta & i = PS \\ \frac{1}{4} M_V^2 f_V^2 (u_\alpha u_\beta - g_{\alpha\beta}) & i = V \end{cases} \quad (31)$$

^cIn case of the B^+ meson the internal decays due to $W^- \rightarrow \bar{u}d$ transitions leads to exactly the same states as the external decays. Nevertheless, we can safely disregard the interference term between the external and internal amplitudes, which is expected to be very small because the total decay widths of the \bar{B}^0 and B^+ mesons coincide with a good accuracy.

Denoting by Γ_{ij} the partial NL width, where the index i refers to a PS or V meson produced in the upper blocks of the diagrams of Fig. 2 and the index j denotes a charmed, resonant or non-resonant, hadron state (D, D^*, X_c) produced in the lower blocks, one gets (cf. also [14])

$$\begin{aligned}
\Gamma_{ij}/\Gamma_0 &= \frac{\pi^2 C_1^2 f_i^2}{2M_B^2} [(1 + \zeta_j)^2 - \zeta_i^2]^2 (\zeta_j^{-1/2} - \zeta_j^{1/2})^2 a(\zeta_i^2, \zeta_j^2) \xi^2(\eta) & i = j = PS \\
\Gamma_{ij}/\Gamma_0 &= \frac{\pi^2 C_1^2 f_i^2}{2M_B^2} (\zeta_j^{-1/2} + \zeta_j^{1/2})^2 a^3(\zeta_i^2, \zeta_j^2) \xi^2(\eta) & i, j = PS, V \text{ or } V, PS \\
\Gamma_{ij}/\Gamma_0 &= \frac{\pi^2 C_1^2 f_i^2}{2M_B^2} [(1 + \zeta_j)^2 - \zeta_i^2] (R_{ij}/\zeta_j) a(\zeta_i^2, \zeta_j^2) \xi^2(\eta) & i = j = V \\
\Gamma_{ij}/\Gamma_0 &= \frac{4\pi^2 C_1^2 f_i^2}{M_B^2} \int_{s_{th}}^{(1-\zeta_i)^2} ds d\vec{p}_\perp |\chi(\tilde{x}_+, p_\perp^2)|^2 \frac{a(\zeta_i^2, s)}{\tilde{x}_+ - \tilde{x}_-} \\
&\quad [\tilde{x}_+(\tilde{x}_+ + \tilde{x}_-)^2 - (\tilde{x}_- + 3\tilde{x}_+) \zeta_i^2] & i = PS; j = X_c \\
\Gamma_{ij}/\Gamma_0 &= \frac{4\pi^2 C_1^2 f_i^2}{M_B^2} \int_{s_{th}}^{(1-\zeta_i)^2} ds d\vec{p}_\perp |\chi(\tilde{x}_+, p_\perp^2)|^2 \frac{a(\zeta_i^2, s)}{\tilde{x}_+ - \tilde{x}_-} \\
&\quad [\tilde{x}_+(\tilde{x}_+ + \tilde{x}_-)^2 - (3\tilde{x}_- + \tilde{x}_+) \zeta_i^2] & i = V; j = X_c
\end{aligned} \tag{32}$$

where $R_{ij} = (1 - \zeta_j^2)^2 - \zeta_i^2[(1 - \zeta_j)^2 - 8\zeta_j]$, $\tilde{x}_\pm = x_\pm(t = \zeta_i^2, s)$ and $s_{th} \equiv M_{th}^2/M_B^2$. The complete list of the partial widths corresponding to *external* NL decays can be found in Ref. [14].

4.2 Internal non-leptonic decays.

The graphs shown in Fig. 3 correspond to the so-called *internal* NL decays of the B -meson. The upper block in Fig. 3(a) represents a hadron state formed by a c -quark resulting from the $b \rightarrow cW^-$ transition and a \bar{u} -quark resulting from the $W^- \rightarrow \bar{u}d$ decay. In Fig. 3(b) the $W^- \rightarrow \bar{c}s$ decay leads to the production of a colourless $c\bar{c}$ state ($\eta_c, J/\psi$ or $c\bar{c}$ in the continuum, $X_{c\bar{c}}$) in the upper block and a strange hadron state ($K, K^*, X_{\bar{d}s}$) in the lower block. The graphs of Fig. 3 correspond to the second term in the VZS Lagrangian (30) and yield, after neglecting QCD corrections, the same factorized expressions already found for the SL decays. The only difference is that we have to replace C_2 for C_1 in Eq. (32) and the factor Γ_0 with $N_c C_2^2 \Gamma_0$ in Eqs. (16) and (27). After these changes the rest of the calculation is essentially the same as in the case of the *external* NL decays.

The diagrams shown in Fig. 6(a) describe the production of a coloured diquark cd and anti-diquark ($\bar{u}\bar{d}$), while the similar graphs in Fig. 6(b) correspond to the production of a cs diquark and a $\bar{c}\bar{d}$ anti-diquark. After making a Fierz-like transformation in Eq. (30) (exchanging the \bar{c} and u quark fields) the VZS Lagrangian can be written in the form

$$\begin{aligned}
L_W^{eff}(\mu = m_b) &= -\frac{4G_F}{\sqrt{2}} V_{cb} V_{ud}^* \left\{ C_- (\bar{c}_L^c \gamma_\mu d_L)^\dagger (\bar{u}_L^c \gamma_\mu b_L)_{3+} \right. \\
&\quad \left. C_+ (\bar{c}_L^c \gamma_\mu d_L)^\dagger (\bar{u}_L^c \gamma_\mu b_L)_{6+} + (d, \bar{u}) \rightarrow (s, \bar{c}) \right\}
\end{aligned} \tag{33}$$

This form suggests that diquarks can be produced in $\bar{3}$ and 3 colour states. The corresponding decay amplitudes are proportional to the factor $C_-/3 \simeq 0.47$. When flying away, diquarks

can pick up the light quark of a $q\bar{q}$ pair produced from the vacuum due to the confinement mechanism. As a result, a colourless charmed baryon $(cd)q$ and a colourless charmless antibaryon $(\bar{u}\bar{d})\bar{q}$ are produced in the B -meson decay (with any number of final mesons). Such a mechanism for the production of baryon-antibaryon states has been firstly suggested in Ref. [38]. The corresponding diagrams are shown in Fig. 6(a), while similar graphs, corresponding to the decay $\bar{B}^0 \rightarrow \Xi_{cs} + \bar{\Lambda}_c$, are depicted in Fig. 6(b).

Instead of calculating many possible channels corresponding to the production of particles both in the upper and lower blocks, we have actually calculated the decay probability for the production of a diquark and anti-diquark with the effective mass $M = \sqrt{q^2}$ and M' larger than the mass of the corresponding baryon. The resulting decay widths are given by Eqs. (27-28) with the replacements $m_\ell \rightarrow M_{\Lambda_c}$ (M_{Ξ_c}) and $M_{th} \rightarrow M_N$ (M_{Λ_c}), obtaining in this way our approximation for the calculation of the inclusive probability of production of baryon-antibaryon states with any number of final mesons.

5 Numerical results.

In what follows we will denote by Γ_{ij} the partial width for the B -meson decays depicted in Fig. 1 for the SL modes and in Figs. 2, 3 and 6 for the NL modes. The index i refers to the lepton pair $\ell\nu_\ell$ or to the hadron states produced in the upper block of the diagrams (π, ρ, \dots , or charmless continuum $X_{\bar{u}d}$ for the diagram 2(a), and $D_s, D_s^*, \dots, X_{\bar{c}s}$ for the diagram 2(b)), while the index j denotes a charmed hadron state (D, D^*, X_c) produced in the lower blocks. The partial width can be written in the form $\Gamma_{ij} = \Gamma_0 \beta_{ij}$, where β_{ij} is a dimensionless quantity and Γ_0 is given explicitly by

$$\Gamma_0 = \frac{G_F^2 M_B^5}{(4\pi)^3} |V_{bc}|^2 = (4.27 \pm 0.44) \cdot 10^{-4} \text{ eV} \quad (34)$$

when the values $|V_{bc}| = 0.039 \pm 0.002$ [5] and $M_B = (5.279 \pm 0.002) \text{ GeV}$ [39] are considered. Then, the total calculated width is given by $\Gamma_B^{tot} = \Gamma_0 \sum_{ij} \beta_{ij}$, where the sum runs over all decay modes of the B -meson. In our phenomenological approach the partial decay widths depend on the following set of parameters:

i) the masses of the constituent quarks building up final mesons and multi-hadrons and the masses of pseudoscalar and vector heavy mesons; the former ones are listed in Table 1, while the latter have been taken from *PDG* [39];

ii) the coupling constants f_{PS} and f_V of the PS and V mesons to the W boson; in units of GeV they are given by (cf. Ref. [14])

$$\begin{aligned} f_\pi &= 0.13 & f_D &= 0.17 & f_{D_s} &= 0.26 & f_{\eta_c} &= 0.38 \\ f_\rho &= 0.20 & f_{D^*} &= 0.20 & f_{D_s^*} &= 0.29 & f_{J/\psi} &= 0.41 \end{aligned} \quad (35)$$

iii) the threshold values M_{th} at which the hadron continuum starts; in our calculations we have adopted the following values (in units of GeV):

$$\begin{aligned} (M_{th})_{c\bar{d}} &= 2.10 & (M_{th})_{c\bar{s}} &= 2.26 & (M_{th})_{c\bar{c}} &= 3.25 \\ (M_{th})_{d\bar{u}} &= 1.00 & (M_{th})_{d\bar{s}} &= 1.06 \end{aligned} \quad (36)$$

for decays into mesons, and

$$(M_{th})_{c\bar{d}} = 1.96 \quad (M_{th})_{c\bar{s}} = 1.65 \quad (M_{th})_{d\bar{u}} = 0.45 \quad (37)$$

for the decays into baryon-antibaryon pair.

The evaluation of the partial widths Γ_{ij} depend upon the form of the b -quark distribution inside the B -meson and, in case of exclusive channels, they depend explicitly upon the IW function $\xi(\eta)$. As described in Section 2, we have used three different models for the B -meson wave function $\chi(x, p_{\perp}^2)$. Two of them, χ_{GI}^{LF} and χ_{NR}^{LF} , are fixed by the choice of the $q\bar{q}$ potential in Eqs. (8) and (9), respectively. The third one is the phenomenological ansatz of Eq. (5), where the parameters $\lambda_0 = 1.0$ and $\xi_0 = m_{sp}/M_B = 0.05$ have been fixed by fitting the *CLEO – II* data [35] (see Fig. 5).

Using these parameters we have calculated the partial widths corresponding to SL (exclusive and inclusive) and NL (external and internal) decay modes; our detailed results, given in terms of Γ_{ij}/Γ_0 , are collected in Tables 2-7. First of all, we want to show that our theoretical estimate of the total B -meson width, Γ_B^{tot} , is consistent with experimental data. Indeed, from Tables 2-7 the sum of all the calculated partial widths Γ_{ij} yields: $0.981 \Gamma_0$ (A), $1.041 \Gamma_0$ (B) and $1.0779 \Gamma_0$ (C). Adding a contribution of $\simeq 3\%$ due to the charmless (direct $b \rightarrow u$ and penguin $b \rightarrow s$) transitions [25], one gets: $\Gamma_B^{tot} = 1.011 \Gamma_0$ (A), $1.071 \Gamma_0$ (B) and $1.107 \Gamma_0$ (C). At $|V_{bc}| = 0.039 \pm 0.002$ [5], one has: $\Gamma_B^{tot} = (4.32 \pm 0.45) \cdot 10^{-4} eV$ (A), $(4.57 \pm 0.47) \cdot 10^{-4} eV$ (B) and $(4.73 \pm 0.49) \cdot 10^{-4} eV$ (C). Our predictions compare favourably with the experimental value $(4.19 \pm 0.11) \cdot 10^{-4} eV$ obtained from the updated world-average value of the \bar{B}^0 -meson life-time, $\tau_{\bar{B}^0} = 1.57 \pm 0.04 ps$ [40].

A summary of our results for the major branching ratios, $\mathcal{B}r_{ij} \equiv \Gamma_{ij}/\Gamma_B^{tot}$, is presented in Tables 8-9 and compared with updated world-average data. Moreover, our results for the inclusive B -meson branching ratios corresponding to the elementary transitions $b \rightarrow c\ell\nu_{\ell}$, $b \rightarrow c\bar{c}s$ and $b \rightarrow c\bar{u}d$ are collected in Table 10. Since the net effect of radiative QCD corrections is expected to be of the same order of magnitude of the uncertainties related to the choice of the B -meson wave function, in Tables 8-10 we have reported also the average of our predictions for cases A , B and C with an assigned error given by the standard deviation from the mean value. It can be seen that a remarkable overall agreement with the data, including the inclusive branching ratio into charmed baryons and the so-called charm counting (i.e., the number of charm quarks produced per b -quark decay), is achieved. A throughout comparison of our results with those of other approaches is out of the scope of this paper. We will limit ourselves to the following two comments.

1. In the parton model [25] the SL branching ratio $\mathcal{B}r_{SL} \equiv \mathcal{B}r(B \rightarrow X_c e \nu_e)$ is $\simeq 13\%$ and the charm counting n_c is $\simeq 1.15$. The inclusion of non-perturbative corrections through the $HQET$ expansion leads only to $\mathcal{B}r_{SL} \gtrsim 12.5\%$ [41]. In Ref. [42] it has been shown that higher-order radiative QCD corrections can increase the partial width of the $b \rightarrow c\bar{c}s$ processes, decreasing in this way the SL branching ratio, but at the price of increasing the charm counting ($n_c \gtrsim 1.25$); moreover, the result for $\mathcal{B}r_{SL}$ turns out to be significantly scale-dependent [5]. Within our phenomenological quark model the calculated SL branching ratio ($\mathcal{B}r_{SL} \simeq 11\%$) is in nice agreement with the updated world-average value 10.90 ± 0.46 [5]. At the same time, our prediction for the charm counting ($n_c \simeq 1.20$) compares favourably with recent experimental results, $n_c^{exp} = 1.16 \pm 0.05$ [43] and $n_c^{exp} = 1.23 \pm 0.07$ [44]. Moreover, our prediction for the inclusive branching ratio due to the elementary $b \rightarrow c\bar{c}s$ transitions, is in accord with experimental findings (see Table 10). Therefore, our results imply that non-perturbative effects, modeled by our B -meson wave function $\chi(x, p_{\perp}^2)$, can enhance significantly the inclusive $b \rightarrow c\bar{u}d$ decay modes, leading to a sizable reduction of the

SL branching ratio without increasing at the same time the charm counting. We point out that a sizable fraction of such an enhancement is provided by *internal NL* decays into heavy mesons and baryon-antibaryon pairs (see Table 7).

2. Our results for exclusive as well as inclusive SL branching ratios are in nice agreement with updated experimental data (see Table 8). It follows that the exclusive SL decays into D and D^* mesons account for $\sim 65\%$ of the total SL branching ratio, leaving a remarkable fraction of $\sim 35\%$ to decays into non- D and non- D^* channels. This is at variance with the result of the *ISGW* model of Ref. [11], which yield only a value of $\sim 10\%$ for the probability of non- D , non- D^* channels.

Before closing, we want to emphasize that the comparison among the electron spectrum calculated within our quark model and the *ISGW* one has been already carried out in Ref. [45], where it has also been shown that our predicted spectrum is consistent with the results obtained in Ref. [46] through a partial *OPE* resummation performed in the end-point region.

6 Conclusions.

A relativistic quark model has been applied to the description of semileptonic and non-leptonic charmed decays of the B -meson. Non-perturbative QCD effects have been mocked up by a constituent quark wave function for the B -meson, describing the motion of the b -quark inside the B -meson. Different approximations for the latter, either based on a phenomenological ansatz or derived from analyses of the meson spectra, have been adopted. In particular, two wave functions, constructed via the Hamiltonian light-front formalism using a relativized and a non-relativistic constituent quark model, have been considered, obtaining a link between standard spectroscopic quark models and the B -meson decay physics.

As for the exclusive semileptonic decay processes $B \rightarrow D l \nu_\ell$ and $B \rightarrow D^* l \nu_\ell$, the universal Isgur-Wise function and the semileptonic branching ratio (as well as the lepton and hadron distributions in the final states) can be calculated in terms of our model B -meson wave function.

A partonic approach has been applied to the description of inclusive B -meson decays to multi-hadrons. Within our approach both the spectra and the decay probabilities can be expressed in terms of the same bound-state wave function used for the description of exclusive semileptonic channels, without any explicit reference to a $1/m_b$ expansion. The main drawback of our approach is likely to be connected with the lack of the effects due to the quark interaction in the final hadronic states. Indeed, our distribution of produced hadron masses has a maximum at the threshold value, i.e., just in the region where quark interaction might be important. Moreover, radiative QCD corrections have been neglected; however, they can be easily introduced using standard methods. Their net effect ($\sim 10 \div 20\%$) is expected to be of the same order of magnitude of the uncertainties related to the choice of the B -meson wave function.

The calculated sum of all the major branching ratios turns out to be close to unity. A remarkable overall agreement with updated world-average data, including the inclusive branching ratio into charmed baryons and the charm counting, has been achieved. In particular, we have found that non-perturbative effects can enhance the inclusive width corresponding to elementary $b \rightarrow c \bar{u} d$ transitions. In this respect an important contribution is provided by *internal* non-leptonic decays into heavy mesons and baryon-antibaryon pairs.

Correspondingly, the semileptonic branching ratio is brought in agreement with its experimental value without increasing, at the same time, the charm counting. Finally, a remarkable fraction ($\sim 35\%$) of semileptonic decay modes have been found to occur in non- D , non- D^* final states.

Acknowledgments.

We are indebted to P. Kulikov for having checked the results of our calculations. Two of the authors (I.L.G. and I.M.N.) acknowledge the financial support of the INTAS grant No. 93-0079. This work was done in part under the RFFR grant, Ref. No. 95-02-04808a.

References

- [1] N. Cabibbo, Phys. Rev. Lett. **10** (1963) 1531. M. Kobayashi and T. Maskawa, Prog. Theor. Phys. **39** (1973) 653.
- [2] M. Danilov, in Proc. Int. Eur. Conf. on High Energy Physics, Marseille (France), 1993, eds. J. Garr and M. Perolett (Edition Frontieres, Gif-sur-Yvette, 1994), p. 551.
- [3] B.Z. Besson, in Proc. of the 16th Int. Symp. on Lepton-Photon Interactions, Ithaca (NY), 1993, eds. P. Drell and D. Rubin, AIP Conf. Proc. n. 392 (AIP, New York, 1994).
- [4] T. Skwarnicki, in Proc. of the 17th Int. Symp. on Lepton-Photon Interactions, Beijing (China), August 1995, eds. Z. Zhi-Peng and C. He-Sheng (World Scientific, Singapore), p. 238. M. Neubert, *ibidem*, p. 298.
- [5] M. Neubert, Int. J. Mod. Phys. **A11** (1996) 4173.
- [6] For a review see, e.g., M. Neubert, Phys. Rep. **245** (1994) 259, and references therein quoted.
- [7] I.I. Bigi, N.G. Uraltsev and A.I. Vainshtein, Phys. Lett. **B247** (1992) 293. I.I. Bigi, M.A. Shifman, N.G. Uraltsev and A.I. Vainshtein, Phys. Rev. Lett. **71** (1993) 496; Int. J. Mod. Phys. **A9** (1994) 2647. A.V. Manohar and M.B. Wise, Phys. Rev. **D49** (1994) 1310. A.F. Falk, M. Luke and M.J. Savage, Phys. Rev. **D49** (1994) 3367. M. Neubert, Phys. Rev. **D49** (1994) 3392 and 4623. B. Block, L. Koyrakh, M.A. Shifman and A.I. Vainshtein, Phys. Rev. **D50** (1994) 3356. T. Mannel, Nucl. Phys. **B413** (1994) 396.
- [8] E.C. Poggio, H.R. Quinn and S. Weinberg, Phys. Rev. **D13** (1976) 1958.
- [9] M. Girone and M. Neubert, Phys. Rev. Lett. **76** (1996) 3061.
- [10] G. Altarelli, G. Martinelli, S. Petrarca and F. Rapuano, Phys. Lett. **B382** (1996) 409.
- [11] (a) D. Scora and N. Isgur: Phys. Rev. **D52** (1995) 2783. (b) N. Isgur: Phys. Rev. **D43** (1991) 810. (c) N. Isgur, D. Scora, B. Grinstein and M.B. Wise: Phys. Rev. **D39** (1989) 799.

- [12] M. Wirbel, B. Stech and M. Bauer: *Z. Phys.* **C29** (1985) 237. M. Bauer, B. Stech and M. Wirbel: *Z. Phys.* **C34** (1987) 103. M. Bauer and M. Wirbel: *Z. Phys.* **C42** (1989) 671.
- [13] F.E. Close and A. Wambach: *Nucl. Phys.* **B412** (1994) 169; *Phys. Lett.* **B349** (1995) 207.
- [14] V.L. Morgunov and K.A. Ter-Martirosyan, *Physics of Atomic Nuclei* **59** (1996) 1221.
- [15] G. Altarelli, N. Cabibbo, G. Corbo, L. Maiani, G. Martinelli, *Nucl. Phys.* **B208** (1982) 365.
- [16] S. Godfrey and N.Isgur, *Phys. Rev.* **D32** (1985) 185.
- [17] I.M. Narodetskii, R. Ceuleener and C. Semay, *J. Phys.* **G18** (1992) 1901.
- [18] E.V. Shuryak, *Phys. Lett.* **93B** (1980) 134; *Nucl. Phys.* **B198** (1982) 83.
- [19] M.B. Voloshin and M.A. Shifman, *Yad. Fiz.* **45** (1987) 463 [*Sov. J. Nucl. Phys.* **45** (1987) 292]; *Yad. Fiz.* **47** (1988) 801 [*Sov. J. Nucl. Phys.* **47** (1988) 512].
- [20] N. Isgur and M.B. Wise, *Phys. Lett.* **232B** (1989) 113; *Phys. Lett.* **237B** (1990) 527.
- [21] J.D. Bjorken, *Phys. Rev.* **179** (1969) 1574. J.D. Bjorken and E.A. Paschos, *Phys. Rev.* **185** (1975) 1964.
- [22] A. Bareiss, C. Peterson and N. Sakai, *Phys. Rev.* **D23** (1981) 2745. A. Bareiss and E.A. Paschos, *Nucl. Phys.* **B327** (1989) 353.
- [23] C.H. Jin, M.F. Palmer and E.A. Paschos, *Phys. Lett.* **329B** (1994) 364.
- [24] A.I. Vainstein, V.I. Zakharov and M.A. Shifman, *Nucl. Phys.* **B147** (1979) 385; *ibidem* 448.
- [25] G. Altarelli and S. Petrarca, *Phys. Lett.* **261B** (1991) 303.
- [26] F.G. Gilman and M.B. Wise, *Phys. Rev.* **D20** (1979) 2392. B. Grinstein, M.J. Savage and M.B. Wise, *Nucl. Phys.* **B319** (1989) 271. A. Buras: *Nucl. Phys.* **B370** (1992) 69.
- [27] M.E. Luke, *Phys. Lett.* **252B** (1990) 447.
- [28] M. Ademollo and R. Gatto, *Phys. Rev. Lett.* **13** (1964) 264.
- [29] A.Yu. Dubin and A.B. Kaidalov, *Yad. Fiz.* **56** (1993) 164.
- [30] For a review see B.D. Keister and W.N. Polyzou, *Adv. Nucl. Phys.* **20** (1991) 225 and F. Coester, *Progress in Part. and Nucl. Phys.* **29** (1992) 1.
- [31] F. Cardarelli, I.L. Grach, I.M. Narodetskii, E. Pace, G. Salmè and S. Simula: *Phys. Lett.* **332B** (1994) 1; *Phys. Rev.* **D53** (1996) 6682. F. Cardarelli, I.L. Grach, I.M. Narodetskii, G. Salmé and S. Simula: *Phys. Lett.* **349B** (1995) 393; *Phys. Lett.* **359B** (1995) 1; *Few-Body Systems Suppl.* **9** (1995) 267.
- [32] S. Simula: *Phys. Lett.* **B373** (1996) 193.

- [33] N.B. Demchuk, I.L. Grach, I.M. Narodetskii and S. Simula, *Phys. of Atom. Nuclei* **59** (1996) 2152. I.L. Grach, I.M. Narodetskii and S. Simula, *Phys. Lett.* **385** (1996) 317.
- [34] ARGUS Collaboration, H. Albrecht et al., *Z. Phys.* **C57** (1993) 533.
- [35] CLEO-II Collaboration, B. Barish et al., *Phys. Rev.* **D51** (1995) 1014.
- [36] ALEPH Collaboration, I. Scott et al., in *Proceedings of the 27th Int. Conf. on High Energy Physics, Glasgow (Scotland), 1994*, eds. P.J. Bussey and J.G. Knowles (IOP, London, 1995).
- [37] A. Buras, J.M. Gerard and R. Ruckl: *Nucl. Phys.* **B268** (1986) 16.
- [38] W.F. Palmer and B. Stech, *Phys. Rev.* **D48** (1993) 4174.
- [39] Particle Data Group, R.M. Barnett et al.: *Phys. Rev.* **D53** (1996) 1.
- [40] T.E. Browder, K. Honscheid and D. Pedrini: preprint UH-515-848-96 / OHSTPY-HEP-E-96-006, hep-ph/9606354, to appear in *Ann. Rev. of Nucl. and Part. Sci.* **46**.
- [41] I. Bigi, B. Blok, M.A. Shifman and A. Vainshtein: *Phys. Lett.* **B323** (1994) 408.
- [42] E. Bagan, P. Ball, V.M. Braun and P. Gosdzinsky: *Phys. Lett.* **B342** (1995) 362.
- [43] CLEO-II Collaboration, Y. Kubota et al.: to appear in the *Proceedings of the 17th Int. Symp. on Lepton-Photon Interactions, Beijing (China), 1995*.
- [44] ALEPH Collaboration, D. Buskulic et al., preprint CERN-PPE/96-117.
- [45] I.L. Grach, I.M. Narodetskii, K.A. Ter-Martirosyan and S. Simula: in *Proc. of the 2nd Int. Conf. on Hyperons, Charm and Beauty Hadrons, Montréal (Canada), 27-30 August 1996*; to appear in *Nucl. Phys. B (Proc. Suppl.)* **55A** (1997), hep-ph/9611427.
- [46] T. Mannel and M. Neubert: *Phys. Rev.* **D50** (1994) 2037.
- [47] L3 Collaboration: preprint CERN-PPE/96-49.

Table 1. Values of the constituent quark masses adopted for our models of the B -meson wave function $\chi(x, p_{\perp}^2)$. Case A is the phenomenological wave function of Eq. (5). Cases B and C correspond to the light-front wave functions χ_{GI}^{LF} and χ_{NR}^{LF} (see Eq. (10)), derived via the LF formalism from the relativized [16] (Eq. (8)) and the non-relativistic [17] (Eq. (9)) constituent quark models, respectively.

Case	m_u	m_s	m_c	m_b
A	0.265	0.560	1.400	5.279
B	0.220	0.419	1.628	4.977
C	0.337	0.576	1.835	5.237

Table 2. Partial widths Γ_{ij} for semileptonic charmed decays of the B -meson in units of Γ_0 (see Eq. (34)). Cases A, B and C correspond to the parameter sets of Table 1. The row labeled Σ correspond to the total semileptonic branching ratio calculated for each final lepton pair.

$j \setminus i$	$e\nu$			$\mu\nu$			$\tau\nu$		
	A	B	C	A	B	C	A	B	C
D	1.83	2.07	1.69	1.82	2.06	1.69	0.56	0.59	0.53
D^*	5.54	5.98	5.26	5.52	5.96	5.24	1.39	1.45	1.34
X_c	3.10	3.99	5.88	3.08	3.97	5.84	0.36	0.47	0.75
Σ	10.47	12.04	12.83	10.42	11.99	12.77	2.31	2.51	2.62

Table 3. Partial widths for the non-leptonic charmed decays of the \bar{B}^0 -meson corresponding to the *external* transition $W^- \rightarrow \bar{u}d$ (see Fig. 2(a)), in units of Γ_0 . The notations are the same as in Table 2.

$j \setminus i$	π^-			ρ^-			$X_{\bar{u}d}^-$		
	A	B	C	A	B	C	A	B	C
D^+	0.40	0.49	0.36	0.90	1.08	0.82	5.96	6.67	5.34
D^{*+}	0.42	0.49	0.38	1.08	1.25	0.99	19.43	20.87	18.51
X_c^+	0.75	0.92	1.26	1.73	2.15	2.96	9.53	12.36	17.93
Σ	1.57	1.90	2.00	3.71	4.48	4.77	34.92	39.90	41.78

Table 4. The same as in Table 3, but for the *external* $W^- \rightarrow \bar{c}s$ transition (see Fig. 2(b)).

$j \setminus i$	D_s^-			D_s^{*-}			$X_{\bar{c}s}^-$		
	A	B	C	A	B	C	A	B	C
D^+	1.55	1.75	1.13	1.28	1.43	1.19	2.42	2.25	2.32
D^{*+}	1.09	1.20	1.02	3.35	3.66	3.15	6.66	5.71	6.46
X_{cd}^+	1.29	1.63	2.44	2.28	3.03	4.58	1.58	1.62	1.18
Σ	3.93	4.58	4.59	6.91	8.12	8.92	10.66	9.58	9.96

Table 5. Partial widths for the *internal* NL charmed decays of the \bar{B}^0 -meson corresponding to the transition $W^- \rightarrow \bar{u}d$ (see Fig. 3(a)), in units of Γ_0 .

	D^0			D^{*0}			$X_{\bar{u}c}$		
	A	B	C	A	B	C	A	B	C
π^0	< 0.01	< 0.01	< 0.01	< 0.01	< 0.01	< 0.01	< 0.01	< 0.01	< 0.01
ρ^0	0.01	0.01	0.01	0.02	0.02	0.01	0.62	0.62	0.43
X_{dd}^0	0.15	0.13	0.16	0.31	0.28	0.34	1.40	0.98	0.98
Σ	0.16	0.14	0.17	0.33	0.30	0.35	2.02	1.60	1.41

Table 6. The same as in Table 5, but for the *internal* $W^- \rightarrow \bar{c}s$ transition (see Fig. 3(b)).

	η_c			J/ψ			$X_{\bar{c}c}^0$		
	A	B	C	A	B	C	A	B	C
K^0	0.02	0.02	0.01	0.01	0.02	0.01	0.06	0.06	0.03
K^{*0}	0.05	0.06	0.05	0.14	0.15	0.12	0.39	0.31	0.12
X_{ds}^0	0.32	0.25	0.34	0.56	0.44	0.60	0.29	0.12	0.04
Σ	0.39	0.33	0.40	0.71	0.61	0.73	0.74	0.49	0.19

Table 7. Values of the inclusive partial widths for the $\bar{B}^0 \rightarrow \bar{N}\Lambda_c + X$ and $\bar{B}^0 \rightarrow \Xi_{cs}\bar{\Lambda}_c + X$ decays (see Fig. 6), in units of Γ_0 .

$\bar{B}^0 \rightarrow \bar{N}\Lambda_c + X$			$\bar{B}^0 \rightarrow \Xi_{cs}\bar{\Lambda}_c + X$		
A	B	C	A	B	C
6.80	4.51	3.86	2.09	1.00	0.31

$B \rightarrow$ baryon + antibaryon

A	B	C
8.89	5.51	4.17

Table 8. B -meson branching ratios ($\mathcal{B}r_{ij} \equiv \Gamma_{ij}/\Gamma_B^{tot}$ given in %) calculated for exclusive and inclusive semileptonic charmed decays of the B -meson.

Decay Mode	A	B	C	average	Exp. data
$\mathcal{B}r(B \rightarrow X_c \ell \nu_\ell)$	10.35	11.24	11.59	11.06 ± 0.64	10.90 ± 0.46 [5]
$\mathcal{B}r(B \rightarrow X_c \tau \nu_\tau)$	2.28	2.34	2.37	2.33 ± 0.05	2.60 ± 0.32 [4]
$\mathcal{B}r(B \rightarrow D e \nu_e)$	1.81	1.93	1.53	1.76 ± 0.21	1.75 ± 0.43 [39]
$\mathcal{B}r(B \rightarrow D^* e \nu_e)$	5.48	5.58	4.75	5.27 ± 0.45	4.93 ± 0.42 [39]

Table 9. The same as in Table 8, but for various exclusive non-leptonic charmed decays of the B -meson.

Decay Mode	A	B	C	average	Exp. data
$\mathcal{B}r(B^0 \rightarrow D^+ \pi^-)$	0.40	0.46	0.34	0.40 ± 0.07	0.31 ± 0.04 [40]
$\mathcal{B}r(B^0 \rightarrow D^+ \rho^-)$	0.89	1.01	0.74	0.88 ± 0.14	0.84 ± 0.17 [40]
$\mathcal{B}r(B^0 \rightarrow D^{*+} \pi^-)$	0.41	0.46	0.34	0.40 ± 0.05	0.28 ± 0.04 [40]
$\mathcal{B}r(B^0 \rightarrow D^{*+} \rho^-)$	1.07	1.17	0.89	1.04 ± 0.14	0.73 ± 0.15 [40]
$\mathcal{B}r(B^0 \rightarrow D^+ D_s^-)$	1.53	1.63	1.02	1.39 ± 0.33	0.74 ± 0.28 [40]
$\mathcal{B}r(B^0 \rightarrow D^+ D_s^{*-})$	1.27	1.33	1.08	1.23 ± 0.13	1.14 ± 0.50 [40]
$\mathcal{B}r(B^0 \rightarrow D^{*+} D_s^-)$	1.08	1.12	0.92	1.04 ± 0.11	0.94 ± 0.33 [40]
$\mathcal{B}r(B^0 \rightarrow D^{*+} D_s^{*-})$	3.31	3.42	2.85	3.19 ± 0.30	2.00 ± 0.64 [40]
$\mathcal{B}r(B \rightarrow \text{charmed baryons})$	8.79	5.15	3.77	5.9 ± 2.6	6.4 ± 1.1 [39] 7.1 ± 1.6 [40]
<i>charm counting</i>	1.22	1.20	1.20	1.20 ± 0.01	1.16 ± 0.05 [43] 1.23 ± 0.07 [44]

Table 10. Inclusive B -meson branching ratios ($\mathcal{B}r_{ij} \equiv \Gamma_{ij}/\Gamma_B^{tot}$ given in %) corresponding to the elementary transitions $b \rightarrow c \ell \nu_\ell$, $b \rightarrow c \bar{c} s$ and $b \rightarrow c \bar{u} d$.

Decay Mode	A	B	C	average	exp. data
$\mathcal{B}r(b \rightarrow c \ell \nu_\ell)$	22.9	24.8	25.5	24.4 ± 1.3	23.08 ± 1.46 [47]
$\mathcal{B}r(b \rightarrow c \bar{c} s)$	25.1	23.1	22.7	23.6 ± 1.3	23.9 ± 3.8 [40]
$\mathcal{B}r(b \rightarrow c \bar{u} d)$	49.0	49.3	49.1	49.1 ± 0.2	

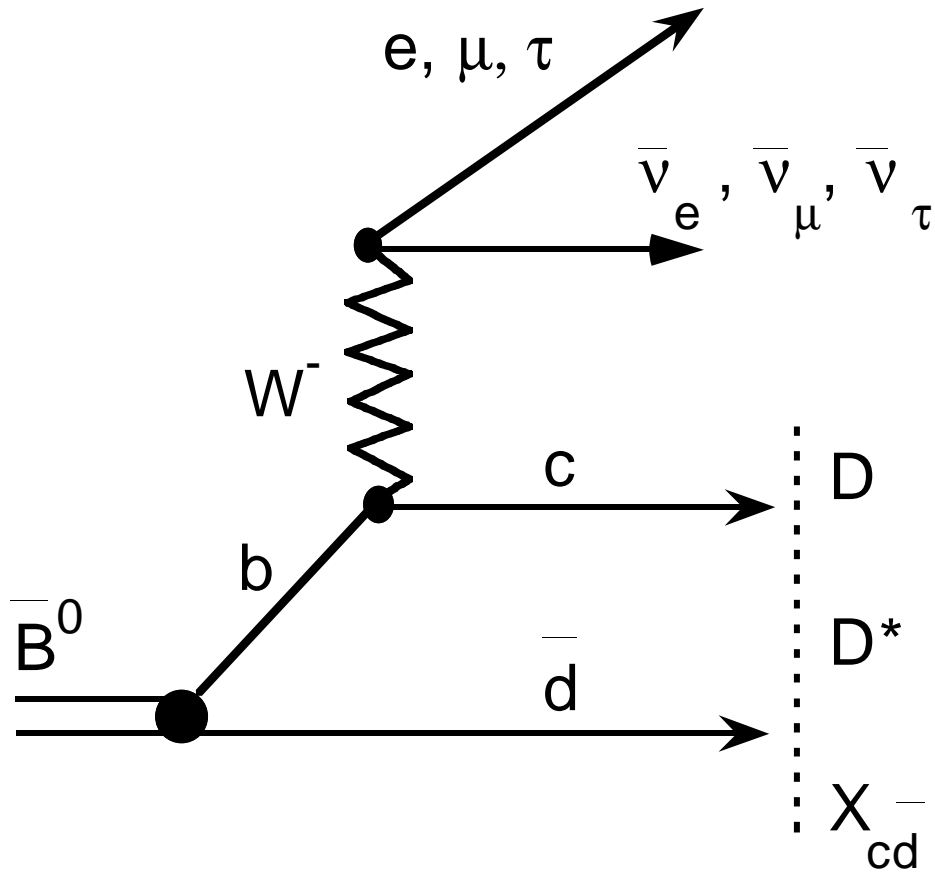


Figure 1. Semileptonic \bar{B}^0 -meson decay modes. The symbol $X_{q\bar{q}}$ stands for mesons with the flavour content of a $q\bar{q}$ pair produced in the continuum.

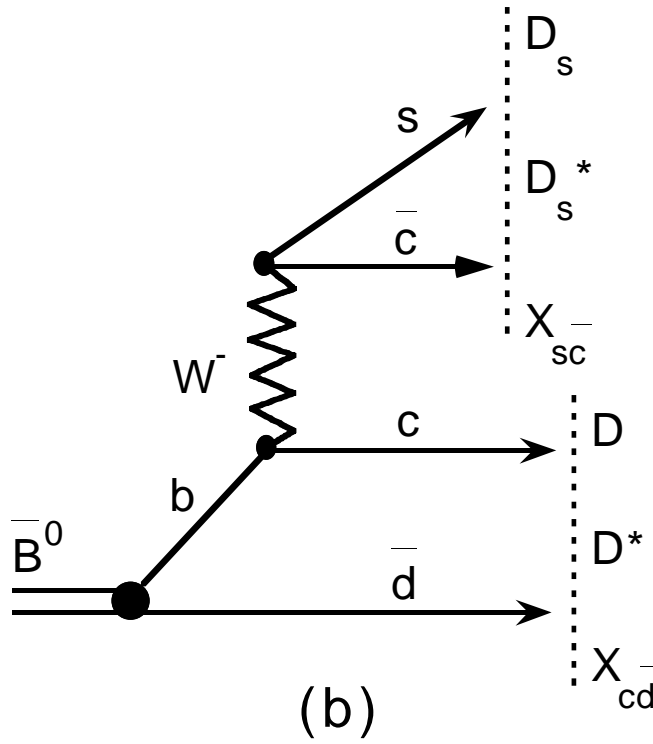
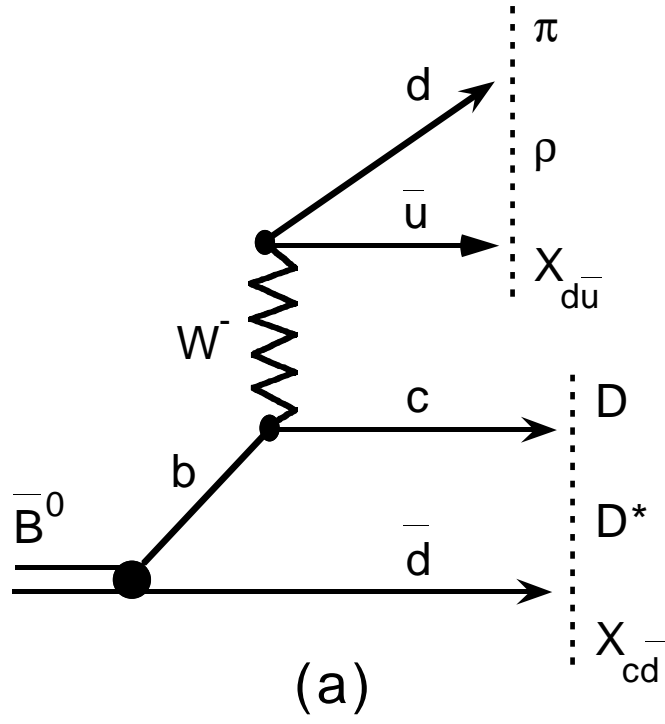


Figure 2. Non-leptonic *external* \bar{B}^0 -meson decay modes, corresponding to $W^- \rightarrow \bar{u}d$ (a) and $W^- \rightarrow \bar{c}s$ (b), respectively.

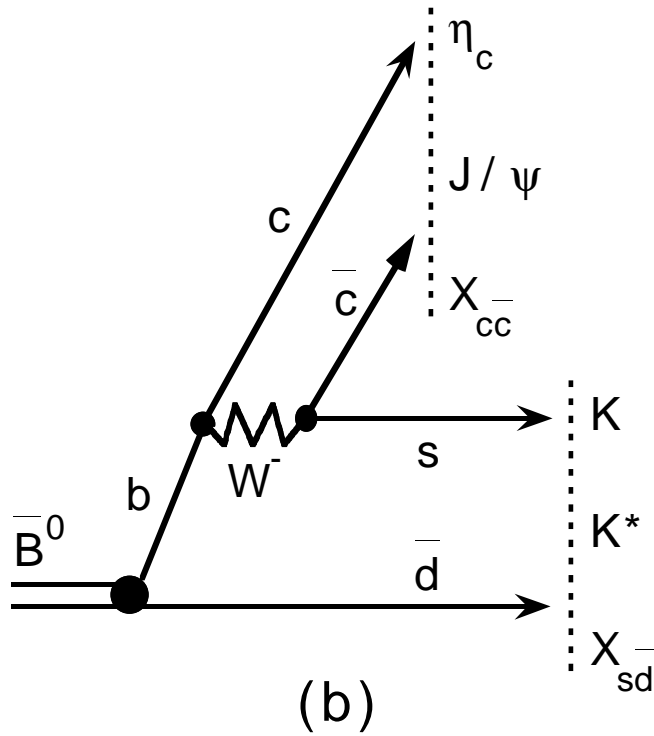
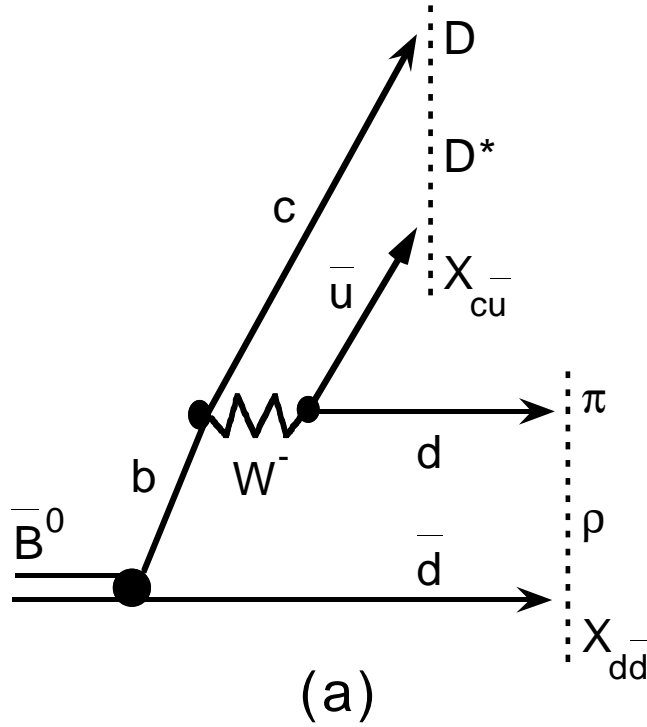


Figure 3. Diagrams of *internal* non-leptonic \bar{B}^0 -meson decays into heavy mesons in case of the $W^- \rightarrow \bar{u}d$ transition (a) and $W^- \rightarrow \bar{c}s$ transition (b).

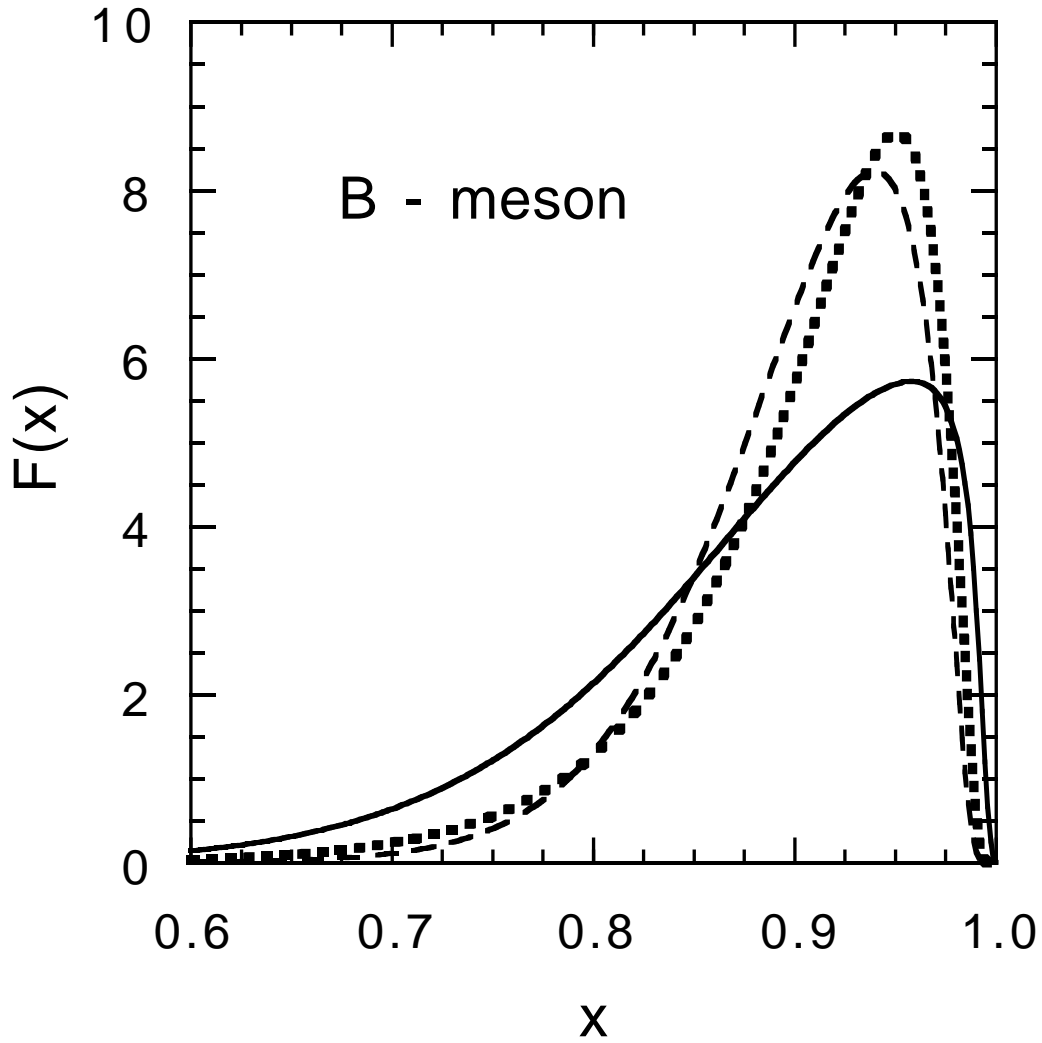


Figure 4. The distribution function $F(x)$ of a b -quark inside the B -meson (Eq. (11)) versus the LF momentum fraction x . The dotted line is the result obtained using the phenomenological ansatz of Eq. (5). The solid and dashed lines correspond to the calculation performed with χ_{GI}^{LF} and χ_{NR}^{LF} , obtained from the solution of Eq. (8) with the relativized interaction of Ref. [16] and the solution of Eq. (9) with the non-relativistic potential of Ref. [17], respectively.

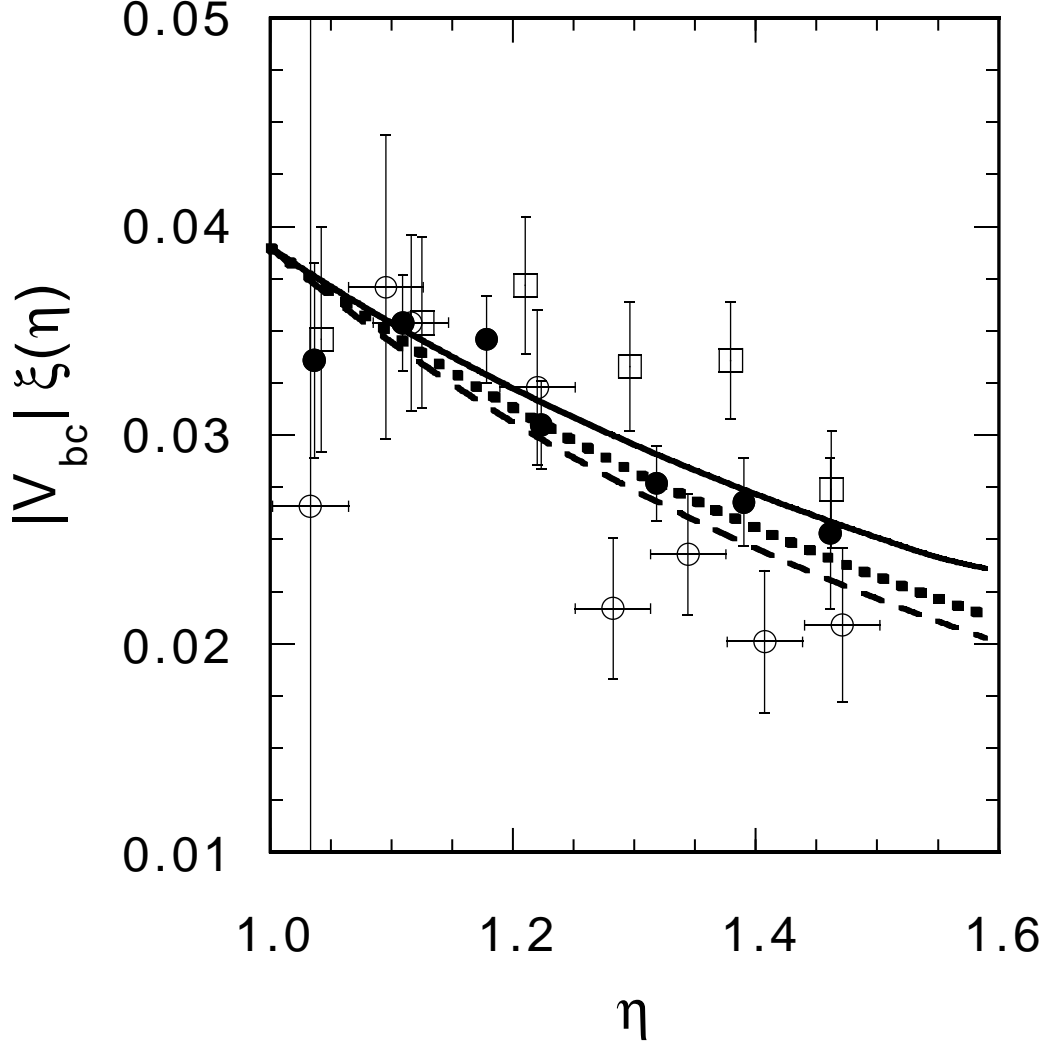
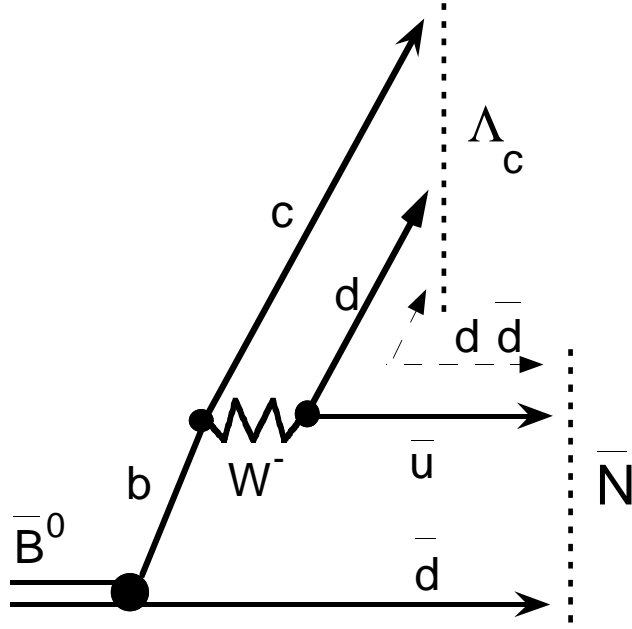
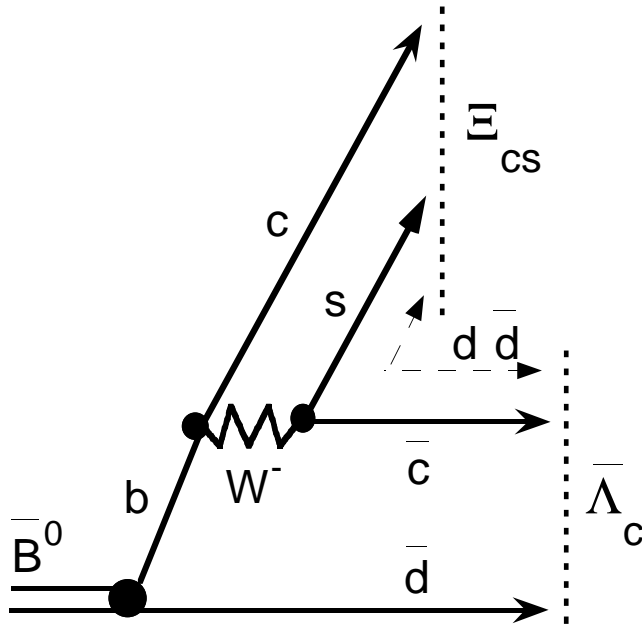


Figure 5. The IW form factor $\xi(\eta)$, times $|V_{bc}|$, as a function of the recoil η . The open dots, full dots and squares correspond to the experimental data of Refs. [34], [35], [36], respectively. The dotted line is the result of the calculations of Eq. (6), times $|V_{bc}| = 0.0390$ [5], obtained using the phenomenological ansatz of Eq. (5). The dashed and solid lines correspond to the results of the calculations of Eq. (4), times $|V_{bc}| = 0.0390$ [5], obtained using the LF wave functions χ_{NR}^{LF} and χ_{GI}^{LF} , respectively.



(a)



(b)

Figure 6. (a) *Internal non-leptonic decays of the \bar{B}^0 -meson into a diquark and an anti-diquark with the creation of one more $q\bar{q}$ light-quark pair in case of the $W^- \rightarrow \bar{u}d$ transition.* (b) *The same as in (a), but for the $W^- \rightarrow \bar{c}s$ transition.*